

# Model and Chattering Free Adaptive Fuzzy SMC for Robotic Manipulator Systems

Maryam Sadeq Ahmed<sup>1</sup>, Ali Hussien Mary<sup>1</sup>, Hisham Hassan Jasim<sup>1</sup>

<sup>1</sup> University of Baghdad  
Al-Khwarizmi College of Engineering  
Department of Mechatronics Engineering

**Annotation:** This In recent decades, many researchers proposed fuzzy Sliding Mode Control (SMC) strategies that aim to eliminate the chattering problem in control of Multi-Input-Multi-Output (MIMO) nonlinear robotics manipulator systems. All these methods impose the need to determine the dynamic model of system under control, which is a challenging task in many practical cases. This paper presents a new model free and chattering free SMC method for MIMO nonlinear robotics manipulator systems based on Proportional-Derivative (PD) and fuzzy logic control. Proposed controller combines the robustness feature of SMC, simplicity of Proportional-Integral-Derivative (PID) control and ability of fuzzy technique in function approximation of discontinuity part of traditional SMC. In this paper, PD control is used as equivalent control in order to stabilize the system while adaptive fuzzy SMC is used to handle uncertainty of the system. Lyapunov's second method is utilised to prove stability of proposed controller. Two different robotic manipulator configurations; two-links with payload and three links robotic manipulator under external disturbance and system uncertainties are simulated to demonstrate the efficiency of the proposed method.

**Keywords:** SMC, Robotics Systems, Fuzzy Control, Trajectory Tracking, lyapunov stability

## 1. Introduction

The complexity of the robot manipulator dynamic, high nonlinearities and strong coupling are making trajectory control task of these systems very difficult [1-5]. Moreover, most of these systems are suffering from system uncertainties and external disturbance which increase the difficulty of the motion control of the robot manipulator systems. Different control schemes had been proposed for this problem such as model predictive control, feedback linearization, and computed torque control. However, these control approaches are model based which means that the dynamic of robot manipulator must be known and this may be difficult in practical applications. Proportional integral derivative (PID) controllers are still widely used in the industrial application due to simplicity in its structure and also in tuning its parameters ([2,3]. Modern control strategies combined with PID controller to increase its ability to dealing with parameter variations, uncertainties and external disturbance for controlling nonlinear systems like robot manipulator. Adaptive control, neural control, and robust control are the most control schemes that used with PID to improve its performance and ensuring its stability and convergence of tracking error for controlling nonlinear systems([4-12]. Sliding mode control is one of the most important nonlinear robust control techniques that applied successfully in control of multivariable nonlinear systems in presence of external disturbance and system uncertainties. The traditional SMC control law consists of two terms, first one is equivalent control term that is based on dynamic model of controlled system and the second one is referred to as discontinuous control. There are two main drawbacks related with traditional SMC. In practical applications, it may not be easy to determine the exact dynamic model of the system due to uncertainties and complexity of system structure; and discontinuous term causes the high frequency chattering problem[13-21]. Chattering can be reduced by using saturation function instead of signum function or by employing a low pass filter in practice. The ability of ANN to approximate the nonlinear function is exploited and used in representation of system dynamics to approximate the sliding mode equivalent control[22]. Based on the method proposed by Roopaei and Jahromi in 2009 that eliminates chattering of SMC, and control scheme presented in[23] that avoids the need to determine dynamic model of

robotic manipulator, this paper proposes a novel control scheme for general MIMO nonlinear robotic manipulator systems that is simple and robust. The main advantages of proposed method are: i) guaranteed robust behaviour of controlled system in presence of system uncertainties and external disturbance; ii) model free design procedure with the control law being based only on error, its derivative and sliding surface; and iii) removal of the chattering problem. This paper is organized as follows: Sec.2 discusses the robotic manipulator dynamic model. Sec. 3 presents the proposed control method. Stability of the proposed method by Lyapunov's second method discussed in Sec.4. in Sec. 5, the theoretical results are used for controlling two links and three link SCARA robot arms and compares its performance with standard SMC subjected to parameter variations and external disturbance. Conclusions are included in Sec.6.

## 2. Robotic Manipulator Dynamic

Dynamic model of a MIMO nonlinear robotic manipulator system can be expressed as follows:

$$M(q)\ddot{q} + N(q, \dot{q})\dot{q} + G(q) + H(\dot{q}) + \tau_d = \tau \quad (1)$$

Where  $q \in R^n$  is joint angular position vector,  $\tau$  is torque vector,  $M(q) \in R^{n \times n}$  is inertia matrix as a function of  $q$ ,  $N(q, \dot{q}) \in R^{n \times n}$  is Coriolis/centripetal vector,  $G(q) \in R^n$  is gravity vector,  $H(\dot{q}) \in R^n$  is frictional force vector and  $\tau_d \in R^n$  is external disturbance. In general, the system dynamics and external disturbance are unknown but they are known to be bounded. The following properties and assumptions about robot dynamics are required [9].

**Property 1.** Symmetry and boundedness of  $M(q)$ :

$$\|M(q)\| \leq k_1 \quad (2)$$

where  $k_1$  is a positive scalar.

**Property 2.** Boundedness of coriolis/ centrifugal.

$$\|N(q, \dot{q})\| \leq k_2 \quad (3)$$

where  $k_2$  is a positive scalar.

**Property 3.** Boundedness of viscous friction

$$\|H(\dot{q})\| \leq k_3\|\dot{q}\| + H_0 \quad (4)$$

where  $k_3$  and  $H_0$  are positive scalars.

**Property 4.** Boundedness of a gravity vector.

$$\|G(q)\| \leq k_4 \quad (5)$$

where  $k_4$  is a positive scalar.

**Property 5.** Boundedness of the external disturbance.

$$\|\tau_d\| \leq D^+ \quad (6)$$

where  $D^+$  is a positive scalar

**Property 6.**

$\dot{M}(q) - 2N(q, \dot{q})$  is skew – symmetric matrix, then,

$$X^T[\dot{M}(q) - 2N(q, \dot{q})]X = 0, X \in R^n \quad (7)$$

**Assumption 1.** The desired trajectories and their derivatives  $q_{di}(t)$ ,  $\dot{q}_{di}(t)$ ,  $\ddot{q}_{di}(t)$  are bounded as follows:

$$|q_{di}(t)| \leq M_{d1i}, |\dot{q}_{di}(t)| \leq M_{d2i}, |\ddot{q}_{di}(t)| \leq M_{d3i}$$

with  $M_{d1i}$ ,  $M_{d2i}$ , and  $M_{d3i}$  being positive constants.

### 3. Proposed Control Scheme

In order to overcome the shortcoming mentioned above, an adaptive FSMC method is proposed as follows (Structure of proposed control scheme is depicted in Fig. 1:

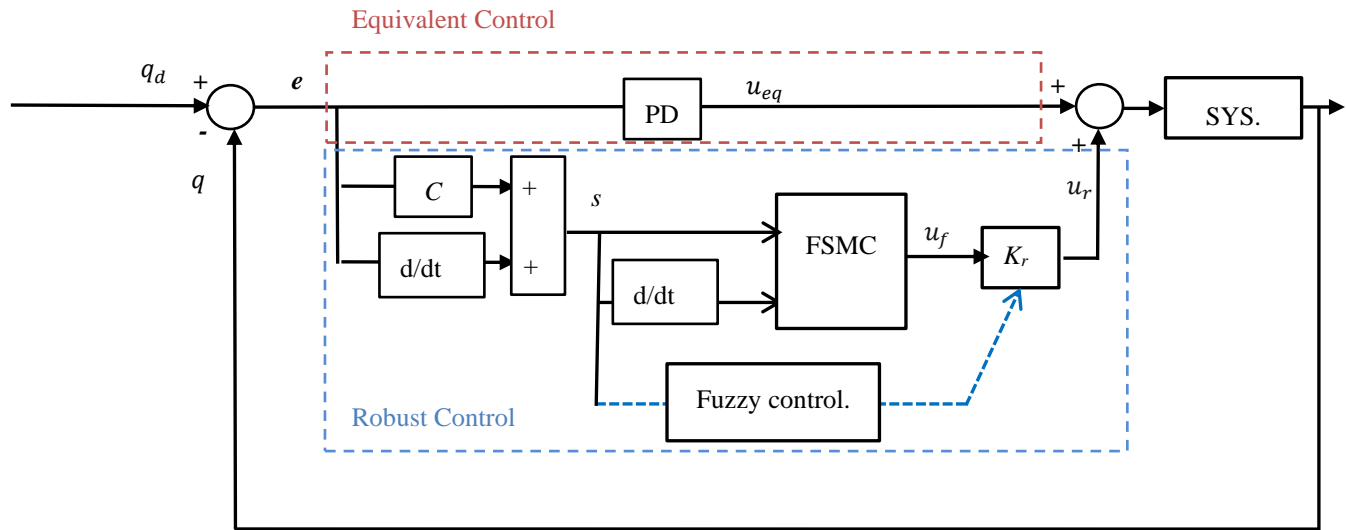


Figure 1 Proposed control scheme

$$\tau = u_{eq} - u_r \quad (8)$$

Where

$$u_{eq} = k_p E + k_d \dot{E} \quad (9)$$

$$u_r = k_r u_f \quad (10)$$

$$E^T = [e_1 \cdots e_n] = [q_{1d} - q_1 \cdots q_{nd} - q_n] \quad (11)$$

$E$  is the tracking error,  $k_r$  represents the normalization factor of output variable and its positive definite diagonal matrix, and  $u_f$  is the output of fuzzy SMC (FSMC).  $k_p$  and  $k_d$  are proportional and derivative positive definite diagonal matrix respectively. Robust control law in (8) is designed as follows:

$$u_f = FSMC(S(t), \dot{S}(t)) \\ = [FSMC(s_1(t), \dot{s}_1(t)), \cdots, FSMC(s_n(t), \dot{s}_n(t))]^T \quad (12)$$

$$s_i(t) = c_i e_i(t) + \dot{e}_i(t) \quad (13)$$

$$S = [s_1, s_2, \cdots, s_n]^T = CE + \dot{E} \quad (14)$$

$$C = \text{diag}(c_1, c_2, \cdots, c_n) \quad (15)$$

Where  $s_i(t)$  are the sliding surfaces and  $c_i$  are positive constants.  $FSMC(S(t), \dot{S}(t))$  refers to the characteristics of fuzzy decision system that is mapping the input linguistic variables  $S(t)$ ,  $\dot{S}(t)$  to the output variable  $u_f$ . The membership functions used are triangular as shown in Fig.2 and they are decomposed into seven fuzzy sets expressed as NB (Negative Big), NM (Negative Medium), NS (Negative Small), Z (Zero), PS (Positive Small), PM (Positive Medium) and PB (Positive Big). 49 fuzzy rules shown in Table 1 are used and intersection minimum and centre average operations are used for fuzzification and

defuzzification, respectively. To improve the performance of closed-loop system and reduce the required control effort, reaching control gain  $k_r$  can be tuned according to the distance of states to the sliding surface. The fuzzy rules of supervisory system that are used to adjust  $k_r$  are developed with one normalized input variable  $s(t)$  and one normalized output variable  $k_f$  where  $k_r = k \cdot k_f$ .  $k$  is a positive definite diagonal matrix and  $k_f = \text{diag}(k_{f1}, \dots, k_{fn})$  is decomposed into four normalized fuzzy sets of Z (Zero), S (Small), M (Medium), and B (Big). The membership functions of inputs and outputs linguistic variables are shown in Fig. 3

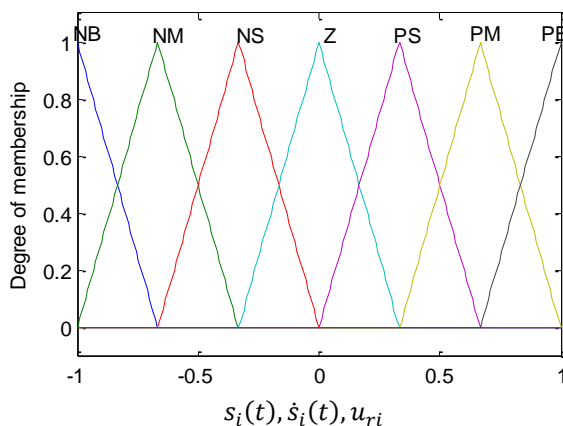


Figure 2 Fuzzy sets for the input variables  $k_{fi}$  and output variables  $s_i(t), \dot{s}_i(t)$

Table 1 49 fuzzy rules

Du(t)		s(t)						
		NL	NM	NS	NE	PS	PM	PL
Ds(t)	NL	NL	NL	NL	NL	NM	NS	ZE
	NM	NL	NL	NL	NM	NS	ZE	PS
	NS	NL	NL	NM	NS	ZE	PS	PM
	NE	NL	NM	NS	ZE	PS	PM	PL
	PS	NM	NS	ZE	PS	PM	PL	PL
	PM	NS	ZE	PS	PM	PL	PL	PL
	PL	ZE	PS	PM	NL	PL	PL	PL

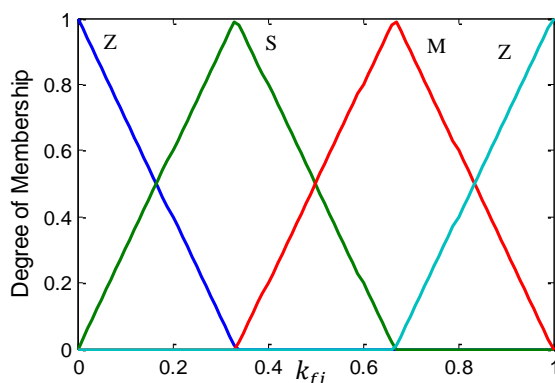


Figure 3 Fuzzy sets for the output variable  $k_{fi}$

The following rules are used to tune  $k_{fi}$ :

- 1) If  $s_i(t)$  is NB or PB then  $k_{fi}$  is B,
- 2) If  $s_i(t)$  is NM or PM then  $k_{fi}$  is M,

3) If  $s_i(t)$  is NS or PS then  $k_{fi}$  is S,

4) If  $s_i(t)$  Z then  $k_{fi}$  is Z.

#### 4. Stability Analysis

Stability analysis of proposed control is executed using Lyapunov's second method with the following positive definite Lyapunov function candidate and its derivative:

$$V = \frac{1}{2} S^T M(q) S \quad (16)$$

$$\dot{V} = S^T M \dot{S} + \frac{1}{2} S^T \dot{M} S = S^T M \dot{S} + S^T N S \quad (17)$$

The dynamic model of the robotic manipulator is linearly parameterized and can be expressed in terms of a nominal reference,  $\dot{q}_r$  [3].

$$Y\phi = M(q)\ddot{q}_r + N(q, \dot{q})\dot{q}_r + G(q) + H(\dot{q}) \quad (18)$$

$$\dot{q}_r = \dot{q}_d + C(q_d - q) \quad (19)$$

where  $Y = Y(q, \dot{q}, \ddot{q}_r, \ddot{q}_r) \in R^{n \times p}$  is the dynamic regression matrix that contains a known nonlinear function,  $\phi \in R^p$  is a vector that contains unknown constant parameters and  $\alpha$  is a positive diagonal matrix.

$$\dot{V} = S^T [M(q)(\ddot{q}_r - \ddot{q}) + N(q, \dot{q})(\dot{q}_r - \dot{q})] \quad (20)$$

$$= S^T [M(q)\ddot{q}_r + N(q, \dot{q})\dot{q}_r + G(q) + H(\dot{q}) + \tau_d - \tau] \quad (21)$$

$$\dot{V} = S^T [Y\phi + \tau_d - \tau] \quad (22)$$

According to properties (2-6) and the result in [12] that stand for bounded desired trajectory  $q_d$ ,

$\|Y\phi\| < \rho(t)$ , where  $\rho(t)$  is a state-dependent function.

$$\dot{V} \leq \|S\|[\rho(t) + D^+] - S^T \tau \quad (23)$$

$$\dot{V} \leq \|S\|[\rho(t) + D^+ + S^T [-k_p E - k_d \dot{E} + k_r u_f]] \quad (24)$$

$$\dot{V} \leq \|S\|[\rho(t) + D^+] + S^T [-k_d (k_d^{-1} k_p E + \dot{E}) + k_r u_f] \quad (25)$$

If we select  $C = k_d^{-1} k_p$ , then (25) becomes

$$\dot{V} \leq \|S\|[\rho(t) + D^+] + S^T [-k_d S + k_r u_f] \quad (26)$$

Let  $\delta(t) = \rho(t) + D^+$ . Fuzzy rules [1] in Table 1 are selected such that  $s_i u_{fi} = -|s_i|$ , then

$$S^T u_r = -[|s_1| + \dots + |s_n|] = -\|S\| \quad (27)$$

With a centroid defuzzification method used for tuning  $k_r$ , the minimum value for  $k_r$  is

$$k_r^{min} = 0.1 k^{min} \quad (28)$$

where

$$k^{min} = \min(k) \quad (29)$$

$$\dot{V} \leq \delta(t)\|S\| - \|k_d\|\|S\|^2 - k_r^{min}\|S\| \quad (30)$$

$$\dot{V} \leq [\|\delta(t)\| - k_r^{min}]\|S\| - \|k_d\|\|S\|^2 \quad (31)$$

If we select  $k_r^{min} > \|\delta(t)\|$ , then  $\dot{V} \leq 0$ , As a result, the nonlinear system under proposed control is globally stable and tracking error converges to zero.

#### 5. Simulation Results

This section demonstrates the effectiveness of the proposed control method via simulation tests. Two different robot manipulators used in this simulation: two links arm with payload and three links CSARA robot to illustrate generality and effectiveness of the proposed method. In order to demonstrate the effectiveness of proposed scheme, it is compared with conventional SMC. Integral Absolute Error (IAE) criterion is used to evaluate effectiveness of control schemes.

$$IAE = \int_0^{t_f} |e(t)| dt \quad (32)$$

### 5.1 Two links robotic manipulator with payload

The following dynamic mode of the two links arm is used in this simulation [24]:

$$\begin{bmatrix} \tau_1 \\ \tau_{21} \end{bmatrix} = \begin{bmatrix} A_{11} & A_{12} \\ A_{12} & A_{21} \end{bmatrix} \begin{bmatrix} \ddot{q}_1 \\ \ddot{q}_2 \end{bmatrix} + \begin{bmatrix} -b\dot{q}_2 & -b\dot{q}_1 - b\dot{q}_2 \\ b\dot{q}_1 & 0 \end{bmatrix} \begin{bmatrix} \dot{q}_1 \\ \dot{q}_2 \end{bmatrix} + \begin{bmatrix} v_1\dot{q}_1 \\ v_2\dot{q}_2 \end{bmatrix} + \begin{bmatrix} p_1 \text{sgn}(\dot{q}_1) \\ p_2 \text{sgn}(\dot{q}_2) \end{bmatrix} + \begin{bmatrix} G_1 \\ G_2 \end{bmatrix} \quad (33)$$

$$A_{11} = I_1 + I_2 + m_1 l_{c1}^2 + m_2 [l_1^2 + l_{c2}^2 + 2l_1 l_{c2} \cos(q_2)] + m_p [l_1^2 + 2l_1 l_2 \cos(q_2) + l_2^2] \quad (34)$$

$$A_{12} = I_2 + m_2 [l_1 l_{c2} \cos(q_2) + l_{c2}^2] + m_p [l_1 l_2 \cos(q_2) + l_2^2] \quad (34)$$

$$A_{12} = A_{21} \quad (35)$$

$$A_{22} = I_2 + m_2 l_{c2}^2 + m_p l_2^2 \quad (36)$$

$$b = m_2 l_1 l_{c2} \sin(q_2) \quad (37)$$

$$G_2 = m_2 l_{c2} g \cos(q_1 + q_2) \quad (38)$$

where  $q_1$  and  $q_2$  are angular positions,  $\tau_1$  and  $\tau_2$  are torques,  $l_1$  and  $l_2$  are lengths,  $I_1$  and  $I_2$  are lengthwise centroid inertia,  $l_{c1}$  and  $l_{c2}$  are distances from the joint,  $m_1$  and  $m_2$  are masses,  $v_1$  and  $v_2$  are coefficients of viscous friction, and  $p_1$  and  $p_2$  are coefficients of dynamic friction of Link1 and Link2, respectively. The parameters of the robotic manipulator are selected as  $m_1 = 1 \text{ kg}$ ,  $m_2 = 1 \text{ kg}$ ,  $l_1 = 1$ ,  $l_2 = 1$ ,  $l_{c1} = .5 \text{ m}$ ,  $l_{c2} = .5 \text{ m}$ ,  $I_1 = .2 \text{ kg m}^2$ ,  $I_2 = .2 \text{ kg m}^2$ ,  $P_1 = P_2 = .1$ ,  $V_1 = V_2 = 0.1$ . The desired joint trajectories in this simulation are selected as  $q_d(t) = [q_{d1} \ q_{d2}]^T$ , where

$$q_{d1} = 0.3 + 0.1 \sin(t) \quad (39)$$

$$q_{d2} = 0.4 + 0.1 \cos(t) \quad (40)$$

The controller parameters selected as follows:

$k_d = \text{diag}(22,22)$ ,  $k_p = \text{diag}(55,55)$  and  $k = \text{diag}(50,50)$ . To demonstrate the robustness and effectiveness of the proposed control method, the dynamic model of the robot manipulator is subjected to external disturbance and also model uncertainties. Moreover, it's compared with the SMC as shown in Figures 4 and 5. In this simulation the parameters of the robot manipulator which include mass, constant friction, and dynamic friction of Link1 and Link2 are changed as much as 15% of their nominal values with disturbance signal  $d = 5 \sin(3t)$ . These figures indicate clearly that the performance of the proposed control method is better than SMC and also with smaller position tracking errors with respect to SMC. Moreover, these figures indicate clearly faster response of the proposed method. The input torque signals of Link1 and, Link2 are shown in Figures 4-c and 5-c. It can be seen form these figures that the same control effort payed form the two methods except a small duration of time at the beginning. Finally, superiority of the proposed control scheme with respect to SMC is approved by calculating IAE as shown in Table 3 that lists the IAE values. This table shows that ability of the proposed control method to reduce tracking error.

### 5.2 Three Links SCARA Robot

The dynamic model of the three link robot manipulator used is as follows [25]:

$$\begin{bmatrix} \tau_1 \\ \tau_2 \\ \tau_3 \end{bmatrix} = \begin{bmatrix} D_{11} & D_{12} & 0 \\ D_{12} & D_{22} & 0 \\ 0 & 0 & D_{33} \end{bmatrix} \begin{bmatrix} \ddot{q}_1 \\ \ddot{q}_2 \\ \ddot{q}_3 \end{bmatrix} + \begin{bmatrix} C_{11} & C_{12} & 0 \\ C_{21} & 0 & 0 \\ 0 & 0 & 0 \end{bmatrix} \begin{bmatrix} \dot{q}_1 \\ \dot{q}_2 \\ \dot{q}_3 \end{bmatrix}$$

$$+ \begin{bmatrix} v_1 \dot{q}_1 \\ v_2 \dot{q}_2 \\ v_3 \dot{q}_3 \end{bmatrix} + \begin{bmatrix} p_1 \operatorname{sgn}(\dot{q}_1) \\ p_2 \operatorname{sgn}(\dot{q}_2) \\ p_3 \operatorname{sgn}(\dot{q}_3) \end{bmatrix} + \begin{bmatrix} G_1 \\ G_2 \\ G_3 \end{bmatrix} + \begin{bmatrix} D_1 \\ D_2 \\ D_3 \end{bmatrix} \quad (41)$$

$$D_{11} = \frac{1}{3} l_1^2 m_1 + \left[ l_1^2 + l_1 l_2 \cos(q_2) + \frac{1}{3} l_2^2 \right] m_2 + (l_1^2 + 2l_1 l_2 + l_2^2) m_3 \quad (42)$$

$$D_{12} = -\left( \frac{1}{2} l_1 l_2 \cos(q_2) + \frac{1}{3} l_2^2 \right) m_2 - (l_1 l_2 + l_2^2) m_3 \quad (43)$$

$$D_{22} = \frac{1}{3} l_2^2 m_2 + l_2^2 m_3 \quad (44)$$

$$C_{11} = -l_1 l_2 \sin(q_2) \dot{q}_2 m_2 - 2l_1 l_2 \sin(q_2) \dot{q}_2 m_3 \quad (45)$$

$$C_{12} = -\frac{1}{2} l_1 l_2 \sin(q_2) \dot{q}_2 m_2 - l_1 l_2 \sin(q_2) \dot{q}_2 m_3 \quad (46)$$

$$C_{21} = -\frac{1}{2} l_1 l_2 \sin(q_2) \dot{q}_1 m_2 - l_1 l_2 \sin(q_2) \dot{q}_1 m_3 \quad (47)$$

where  $q_1$ ,  $q_2$  and  $q_3$  are angular positions,  $\tau_1$ ,  $\tau_2$  and  $\tau_3$  are torques,  $l_1$ ,  $l_2$  and  $l_3$  are lengths,  $m_1$ ,  $m_2$  and  $m_3$  are masses,  $v_1$ ,  $v_2$  and  $v_3$  are coefficients of viscous friction, and  $p_1$ ,  $p_2$  and  $p_3$  are coefficients of dynamic friction of Link1, Link2 and Link3, respectively.

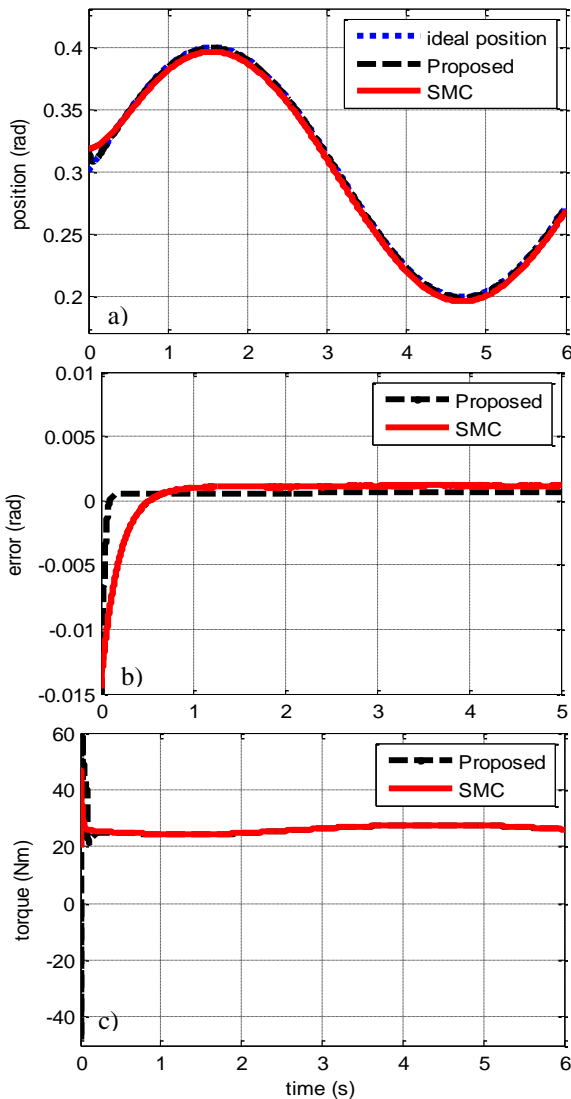


Figure 4. two link tracking position (a), tracking error (b), input torque (c) of link 1

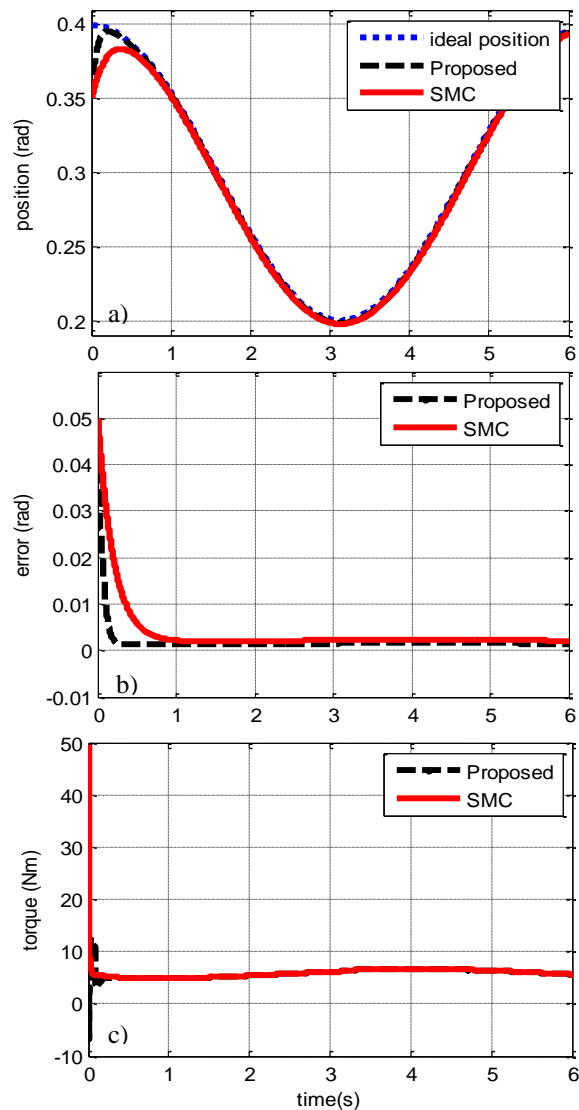


Figure 5. two link Tracking position (a), tracking error (b), input torque (c) of link 2

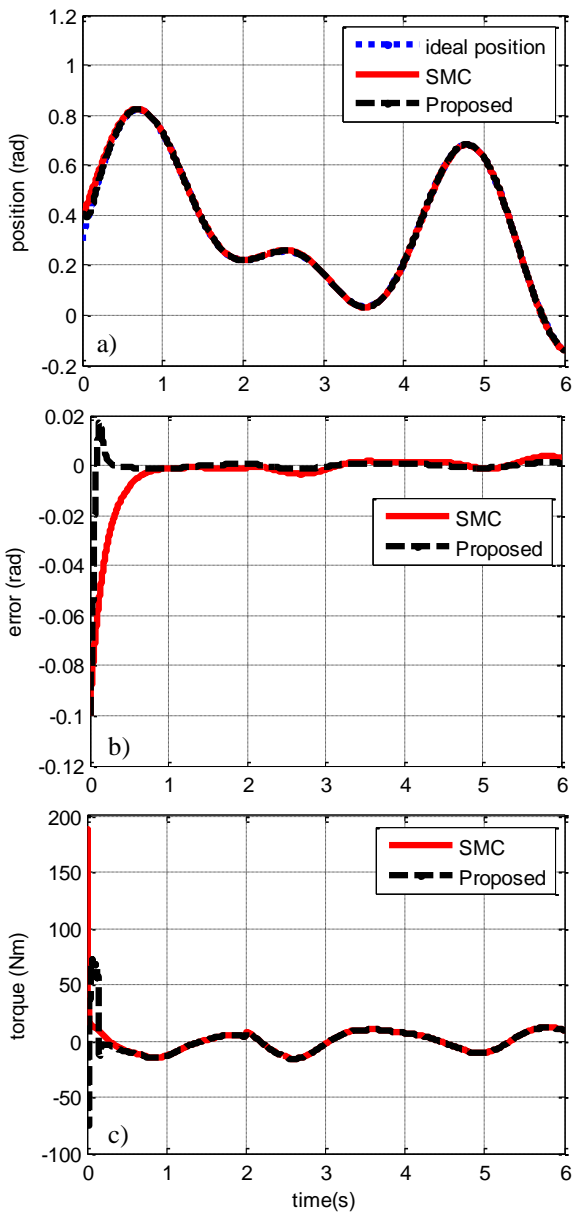


Figure 6 three link tracking position (a), tracking error (b), input torque (c) of link 1

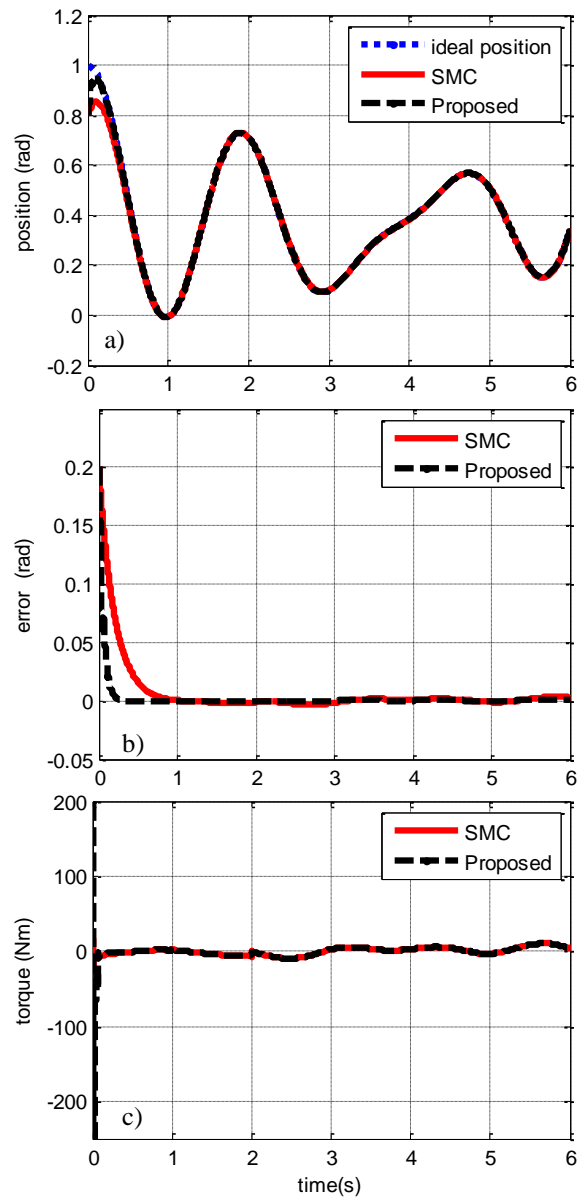


Figure 7 three link tracking position (a), tracking error (b), input torque (c) of link 2



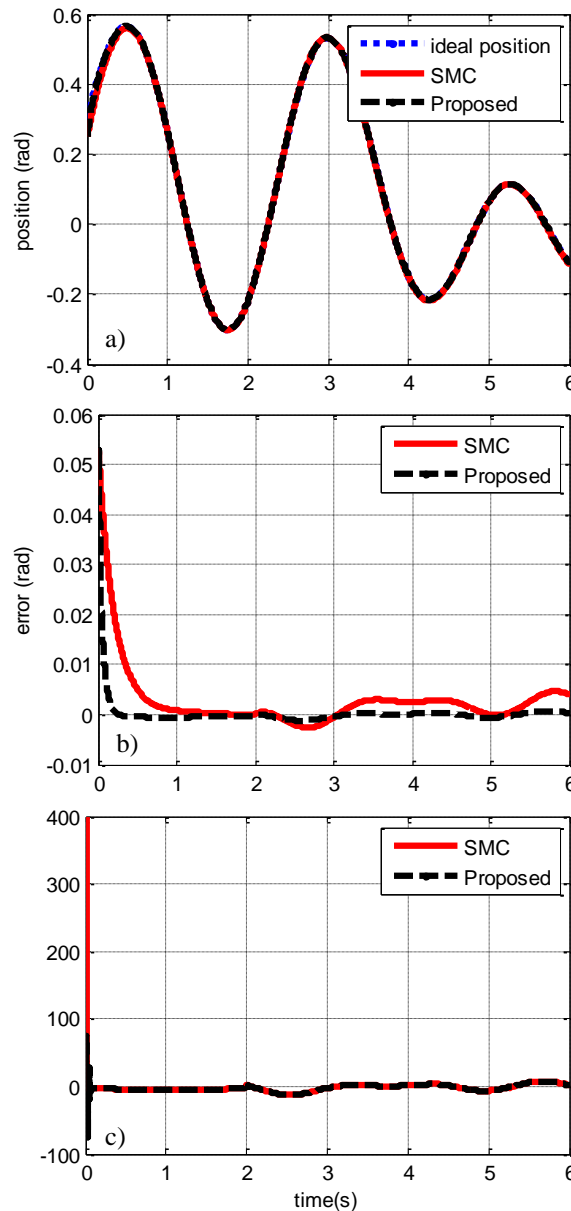


Figure 8. three link tracking position (a), tracking error (b), input torque (c) of link 3

The parameters of the robotic manipulator are selected as  $m_1 = 1 \text{ kg}$ ,  $m_2 = 0.8 \text{ kg}$ ,  $m_3 = 0.5 \text{ kg}$ ,  $P_1 = P_2 = P_3 = 12$ ,  $V_1 = V_2 = V_3 = 0.2$  [14]. The desired joint trajectories in this simulation are selected as  $q_d(t) = [q_{d1} \ q_{d2} \ q_{d3}]^T$

where

$$q_{d1} = 0.3 + 0.1 \sin(t) + .3 \sin(1.7t) + .2\sin(2.9t) \quad (48)$$

(67)

$$q_{d2} = 0.4 + 0.1 \cos(t) + .3 \sin(2.9t) + .2\sin(3.7t) \quad (49)$$

$$q_{d3} = 0.1 + 0.1 \sin(t) + .2 \sin(1.8t) + .3\sin(3.7t) \quad (50)$$

The controller parameters selected for this manipulator as follows:

$$k_d = \text{diag}(30,30,30), k_p = \text{diag}(500,500,500), k = \text{diag}(500, 500,500)$$

Parameters of the robot manipulator dynamic are changed to 14% of their nominal values with external disturbance  $d = 5\sin(3t)$ .

The simulation results that obtained when the proposed method and SMC used for controlling three links SCARA robot manipulator conform the result that obtained when two link robot manipulator used in the test. Tracking position and tracking error for link1, link2 and link3 are shown in Figures 2,3 and 4 respectively. These figures show faster response of the proposed method and also very small position error with respect the SMC which can be also justified based on the *IAE* values that listed in the Table 3. Figures 2,3 and 4 show the control signals for the Link1, Link2 and Link3 respectively.

## 6. Conclusion

In this paper, a model and chattering free adaptive fuzzy SMC scheme for nonlinear robotic manipulator systems with uncertainty in system dynamics in presence of the external disturbance has been proposed. The proposed control method does not require determining the dynamic model of the controlled system with adaptive switching gain to eliminate the chattering problem. Proposed scheme's performance is justified and compared it with the standard SMC by applying them for controlling two links and three links SCARA robot arm.

## References

1. Ahmed MS, Mary AH, Jasim HH. Robust Computed Torque Control for Uncertain Robotic Manipulators. Al-Khwarizmi Engineering Journal. 2021 Sep 29;17(3):22-8.
2. Craig, John J. "Introduction to Robotics." (2005).
3. Mary, A.H., Kara, T. and Miry, A.H., 2016, May. Inverse kinematics solution for robotic manipulators based on fuzzy logic and PD control. In 2016 Al-Sadeq International Conference on Multidisciplinary in IT and Communication Science and Applications (AIC-MITCSA) (pp. 1-6). IEEE.
4. T. Kara, AH. Mary, Robust trajectory tracking control of robotic manipulators based on model-free PID-SMC approach, Journal of Engineering Research. 6(3),(2018).
5. Kara, T. and Mary, A.H., 2018. Feedback-based IKP solution with SMC for robotic manipulators: the SCARA example. International Advanced Researches and Engineering Journal, 2(1), pp.27-32.
6. Eker I. Sliding mode control with PID sliding surface and experimental application to an electromechanical plant. ISA transactions. 2006 Jan 1;45(1):109-18.
7. Sharma R, Gaur P, Mittal AP. Design of two-layered fractional order fuzzy logic controllers applied to robotic manipulator with variable payload. Applied Soft Computing. 2016 Oct 1;47:565-76.
8. Mary AH, Miry AH, Miry MH. An Optimal Robust State Feedback Controller for the AVR System-Based Harris Hawks Optimization Algorithm. Electric Power Components and Systems. 2021 May 7;48(16-17):1684-94.
9. Mary AH, Miry AH, Miry MH. System uncertainties estimation based adaptive robust backstepping control for DC DC buck converter. International Journal of Electrical and Computer Engineering. 2021 Feb 1;11(1):347..
10. Pratumsuwan P, Thongchai S, Tansriwong S. A hybrid of fuzzy and proportional-integral-derivative controller for electro-hydraulic position servo system. Energy Research Journal. 2010;1(2):62-7.
11. Alwan HM, Rashid ZH. Motion Control of Three Links Robot Manipulator (Open Chain) with Spherical Wrist. Al-Khwarizmi Engineering Journal. 2019 May 12;15(2):13-23.
12. Mary AH, Miry AH, Miry MH. ANFIS Based Reinforcement Learning Strategy for Control A Nonlinear Coupled Tanks System. Journal of Electrical Engineering & Technology. 2021 Apr 26:1-9.

13. Nunes EV, Hsu L. Global tracking for robot manipulators using a simple causal PD controller plus feedforward. *Robotica*. 2010 Jan;28(1):23-34..
14. Ranjani M, Temel T, Ashrafiun H. Sliding-mode control approach for faster tracking. *Electronics letters*. 2012 Jul 30;48(15):916-7.
15. Shimizu T, Tadakuma K, Watanabe M, Abe K, Konyo M, Tadokoro S. Permanent-magnetically Amplified Brake Mechanism Compensated and Stroke-Shortened by a Multistage Nonlinear Spring. *IEEE Robotics and Automation Letters*. 2022 Jan 14.
16. Sharma R, Gaur P, Mittal AP. Design of two-layered fractional order fuzzy logic controllers applied to robotic manipulator with variable payload. *Applied Soft Computing*. 2016 Oct 1;47:565-76.
17. Raza F, Zhu W, Hayashibe M. Balance Stability Augmentation for Wheel-Legged Biped Robot Through Arm Acceleration Control. *IEEE Access*. 2021 Apr 5;9:54022-31.
18. Miry AH, Mary AH, Miry MH. Improving of Maximum Power Point Tracking for Photovoltaic Systems Based on Swarm Optimization Techniques. *INOP Conference Series: Materials Science and Engineering 2019 May (Vol. 518, No. 4, p. 042003)*. IOP Publishing.
19. Haddad SQ, Akkar HA. Intelligent swarm algorithms for optimizing nonlinear sliding mode controller for robot manipulator. *International Journal of Electrical & Computer Engineering (2088-8708)*. 2021 Oct 1;11(5).
20. Quang NP, Quang NH. Impact analysis of actuator torque degradation on the IRB 120 robot performance using Simscape-based model. *International Journal of Electrical & Computer Engineering (2088-8708)*. 2021 Dec 1;11(6).
21. Kara T, Mary AH. Adaptive PD-SMC for Nonlinear Robotic Manipulator Tracking Control. *Studies in Informatics and Control*. 2017 Mar 1;26(1):49-58.
22. AH. Mary, T. Kara, Robust proportional control for trajectory tracking of a nonlinear robotic manipulator: LMI optimization approach. *Arabian Journal for Science and Engineering*, 41(12),(2016),5027-36.
23. Miry M. Nonlinear state feedback controller combined with RBF for nonlinear underactuated overhead crane system. *Journal of Engineering Research*. 2021 Sep 2;9(3A).
24. Mary, A., Miry A., Miry M., Kara, T., Nonlinear state feedback controller combined with RBF for nonlinear underactuated overhead crane system. *Journal of Engineering Research*. 2021 Sep 2;9(3A).
25. Roopaei M, Jahromi MZ. Chattering-free fuzzy sliding mode control in MIMO uncertain systems. *Nonlinear Analysis: Theory, Methods & Applications*. 2009 Nov 15;71(10):4430-7..
26. Sharma R, Gaur P, Mittal AP. Performance analysis of two-degree of freedom fractional order PID controllers for robotic manipulator with payload. *ISA transactions*. 2015 Sep 1;58:279-91.
27. Wai RJ, Tu CY, Hsieh KY. Adaptive tracking control for robot manipulator. *International journal of systems science*. 2004 Sep 1;35(11):615-27.